Chemical Physics 143 (1990) 97–107
North-Holland

SPECTRAL CHARACTERISTICS OF THREE DIFFERENT ISOMERIC 2-(AMINOPHENYL)BENZOXAZOLES: EFFECT OF SOLVENTS AND ACID CONCENTRATIONS

Joy Krishna DEY and Sneh K. DOGRA
Department of Chemistry, Indian Institute of Technology, Kanpur - 208016, India

Received 25 April 1989; in final form 14 December 1989

Spectral characteristics of 2-(2′-aminophenyl)-, 2-(3′-aminophenyl)- and 2-(4′-aminophenyl)benzoxazoles (*o*-APBO, *m*-APBO, *p*-APBO respectively) have been studied in solvents of different polarity and hydrogen bond forming ability and at various acid concentrations. The infrared, ultraviolet and fluorescence spectra and low pK_a value for the monocation–neutral equilibrium indicate the presence of intramolecular hydrogen bonding in *o*-APBO. Stokes shifts in different solvents have indicated that *m*-APBO is more polar than *p*-APBO in the S_1 state compared to the S_0 state. Only three prototropic species (dication, monocation and neutral) are observed in the ground state, whereas five prototropic species (dication, non-fluorescent monocation (2′), monocation (2), neutral and non-fluorescent monoanion) are present in the S_1 state. Biprotonic phototautomerism is observed in the monocations of all the molecules. MO calculations (PPP) have also been used to aid in the interpretation of certain experimental results.

1. Introduction

It is well established that intra- and intermolecular hydrogen bonding can lead to large changes in fluorescence spectrum and fluorescence quantum yield (ϕ_f). It has been found that excited-state intramolecular proton transfer (ESIPT) plays a major role in increasing the rate of internal conversion [1–5]. Since the energy barrier for ESIPT is very small [6–9] the rate of phototautomerization is very high ($10^{12}\ s^{-1}$) [10–12]. The phototautomer has a broad fluorescence band with large Stokes shift compared to its normal fluorescence band. The presence of dual fluorescence depends upon the enthalpy of excited-state reaction. In some cases only a large Stokes-shifted fluorescence and in other systems a dual fluorescence is observed. Systems of this type have been widely used as effective light protectors as well as materials in continuous lasers [13–15].

Our present study is concentrated on three molecules, 2-(2′-aminophenyl)-, 2-(3′-aminophenyl)-, and 2-(4′-aminophenyl)benzoxazole. The structure of molecule I (see scheme 1) is such that it will have intramolecular hydrogen bonding (IHB) in the ground state and thus may have a profound effect on the luminescence and photochemical properties of *o*-APBO.

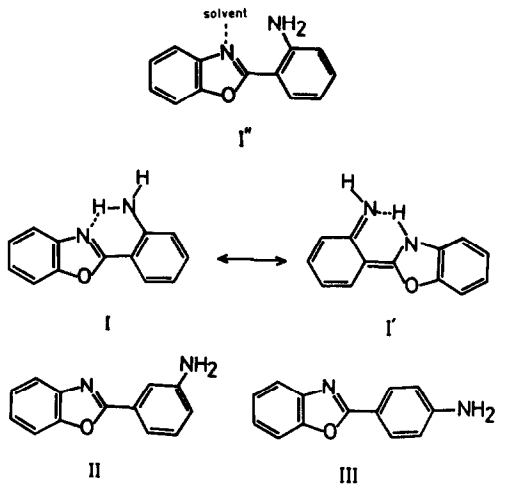

Scheme 1.

Depending on the changes in charge densities at the basic centres on excitation both *m*-APBO and *p*-APBO can give rise to biprotonic and *o*-APBO to a monoprotonic phototautomerism. Earlier studies

have established that the monocations are formed by protonation at the pyridinic nitrogen atom in aminopyridines [16] and aminobenzimidazoles [17,18] and at the amino group in aminoindazoles [19].

The aims of our present study are (i) to observe whether monoprotonic phototautomer is formed in *o*-APBO or not, (ii) to find the site of protonation in the monocations and the dications of the molecules under study, (iii) to determine the pK_as for various prototropic reactions in S_0 and S_1 states and (iv) to perform a quantum chemical calculation (PPP method) to explain the electronic absorption spectra of the molecules and to calculate the charge densities at the basic centres.

2. Materials and methods

The compounds *o*-APBO, *p*-APBO and *m*-APBO were prepared and purified as reported in the literature [20]. Melting point, TLC and excitation spectra were used to establish the purity of the compounds. Analytical grade cyclohexane (SDS), dioxane (Merck), acetonitrile (Merck) and methanol (BDH) were further purified as described elsewhere [21]. Triply distilled water was used for studies in aqueous medium. KOH, H_2SO_4 and ortho-H_3PO_4 used were of analytical grade. The preparation of solutions, equipments used and the method of calculations followed have already been described in recent papers [22–26]. Concentration of solutions was of the order of $\approx 10^{-5}$ M. The aqueous solutions were made in water–methanol mixture containing not more than 0.5% (v/v) methanol.

3. Results and discussions

3.1. Effect of solvents

Fig. 1 depicts the absorption and fluorescence spectra of the molecules in various solvents and at different acid concentrations. The absorption and fluorescence spectral data are compiled in tables 1 and 2 respectively. The absorption spectrum of *m*-APBO is similar to that of 2-phenylbenzoxazole [27] (PBO) and 2-(3′-methylphenyl)benzoxazole [28] except the appearance of a shoulder at 325 nm to the major band (291 nm). The absorption spectrum of *p*-APBO is structured with the λ_{max} at 316 nm. The structure is lost with the increase of solvent polarity. In case of *o*-APBO a large red-shifted band at 365 nm in addition to the normal absorption bands in other molecules is observed. The absorption band maxima in all the cases are red shifted and blue shifted with the increase of polarity of the solvents and with an increase in the capability of hydrogen bond (HB) formation respectively.

Unlike *m*-APBO and *o*-APBO, the fluorescence spectrum of *p*-APBO is structured and the structure is lost with an increase of solvent polarity. The fluorescence band maximum in contrast to the absorption spectrum in all the cases is red shifted in going from cyclohexane to water. The band maxima in cyclohexane are in the order *o*-APBO > *m*-APBO > *p*-APBO but in polar solvents the order has changed to *m*-APBO > *o*-APBO > *p*-APBO. The Stokes shift (table 3) in cyclohexane for *m*-APBO is greater than those of the other molecules and it becomes very large (≈ 10000 cm^{-1}) in water. Fluorescence quantum yield (ϕ_f) of *p*-APBO is nearly unity in all the solvents, whereas those of *m*-APBO and *o*-APBO are small and respectively decrease and increase with the increase of polarity and proton accepting ability of the solvents. Unlike 2-(2′-aminophenyl)-benzimidazole [29] (*o*-APBI), 2-(2′-hydroxyphenyl)benzimidazole [30] (*o*-HPBI), 2-(2′-hydroxyphenyl)benzoxazole [31] (*o*-HPBO) and other similar compounds, only one fluorescence band is observed in *o*-APBO, which does not have large Stokes shift.

Theoretical studies [32] as well as the absorption and fluorescence spectra of benzoxazole (BO) and its alkyl derivatives [33,34] have clearly indicated that the long wavelength transition is localized mainly on the benzene ring and the short wavelength one on the oxazole ring. Brocklehurst [35], Nurmukhamalov et al. [36] and Dey and Dogra [28] have also shown that in case of 2-phenyl derivatives of BO, the phenyl ring acts as the main chromophore and their spectral characteristics are perturbed by the BO moiety. The data of tables 1 and 4, further, substantiate the above results. The change in the band shape, presence of vibrational structure, large red shift and high molar extinction coefficient of the long wavelength absorption band of *p*-APBO compared to *o*-

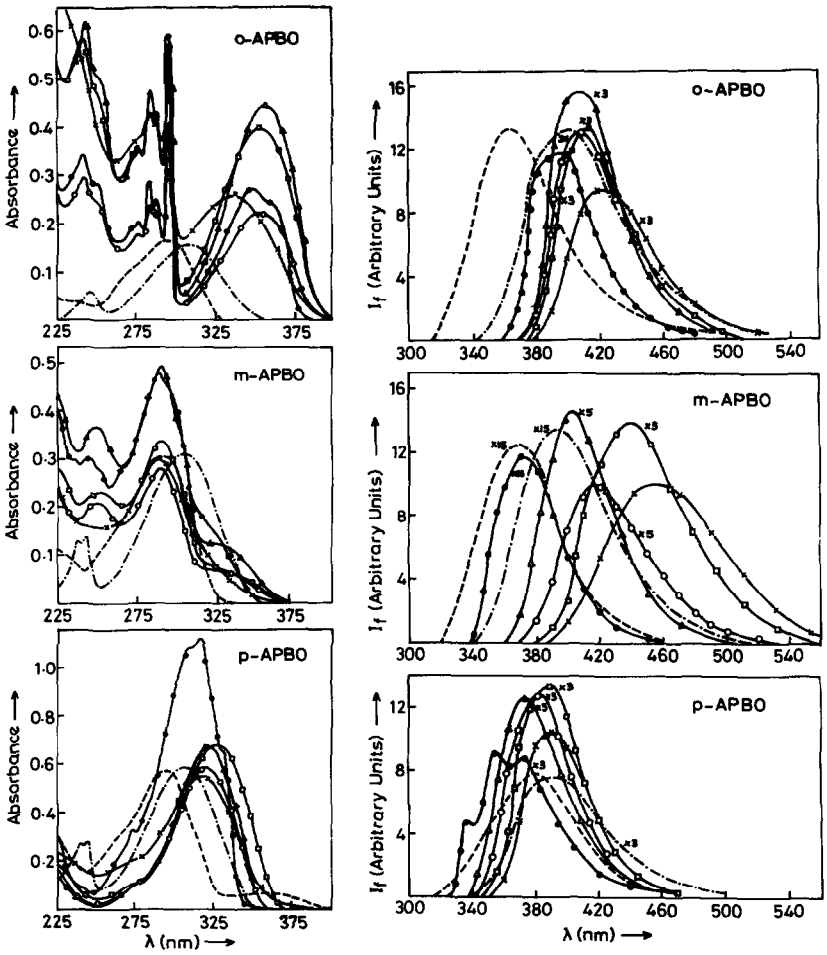

Fig. 1. Absorption and fluorescence spectra of *o*-APBO, *m*-APBO and *p*-APBO in cyclohexane (-●-), dioxane (-△-), acetonitrile (-○-), methanol (-□-) and water (-×-) and their corresponding prototropic species, e.g. monocation (---) and dication (-·-).

APBO or *m*-APBO could be due to the extended conjugation by the amino group at the para position or the presence of dipolar structure III′ as shown in scheme 2. Very high fluorescence quantum yield and small Stokes shift clearly indicate that the geometry of *p*-APBO in the S_1 state is not different from that in the S_0 state. The similar behaviour is also observed

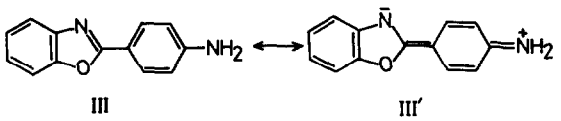

III III′

Scheme 2.

in 2-(4′-aminophenyl)- [18] and 2-(4′-hydroxyphenyl)benzimidazoles (*p*-APBI, *p*-HPBI).

The longest wavelength absorption band system (348 and 365 nm) of *o*-APBO can be a result of intramolecular HB formation. The presence of intramolecular hydrogen bonding in *o*-APBO is confirmed from the decrease in the symmetrical stretching frequency of -N-H bond (3490, 3320 cm^{-1} in *o*-APBO and 3500, 3400 cm^{-1} in *p*-APBO). The small decrease in the symmetrical stretching frequency indicates that intramolecular hydrogen bonding is not very strong. Similar results have also been observed by Merrill and Bennett [1]. The infrared spectra were recorded in CCl_4 solution and band

Table 1
Absorption band maxima (nm) and molar extinction coefficients of 2-(aminophenyl)benzoxazoles in different solvents and at various acid concentrations

Solvent	o-APBO		m-APBO		p-APBO	
	λ_{max}	log ε_{max}	λ_{max}	log ε_{max}	λ_{max}	log ε_{max}
cyclohexane	365	4.15	325	–	325	–
	348	–	291	4.15	316	–
	297	4.32	248	3.95	308	–
	289	4.12		–	284	
	285	4.18			274	
	277	4.03			264	
	242	4.26				
dioxane	367	4.17	330	–	330	–
	352	–	294	4.40	323	4.57
	297	4.30	255	4.28	275	3.85
	290	4.15				
	285	4.19				
	278	4.07				
	244	4.31				
acetonitrile	354	4.16	318	–	322	4.58
	296	4.29	293	4.34	270	sh
	288	4.15	254	4.21		
	284	4.19				
	277	4.06				
	243	4.28				
methanol	354	4.11	318	–	327	4.59
	296	4.28	294	4.35	280	sh
	288	4.14	255	4.18	272	sh
	284	4.18				
	277	4.06				
	242	4.27				
water	337	–	316	–	317	
(pH 6.2)	295	–	291	4.7	272	sh
	284	–				
monocation	299	4.27	313(sh)	–	365	3.34
	290		295	4.31	295	4.29
dication	310	4.25	316(sh)	4.31	307	4.33
	247	3.85	308	3.97	246	4.02
			247		242	4.00

maxima were independent of concentration. In all the solvents the emission maximum for o-APBO occurs around 400 nm. The relatively small Stokes-shifted (3740–5000 cm^{-1}) emission can be assigned to non-proton-transferred form of o-APBO (I or I″) because the proton transferred form (I′) emits fluorescence with large Stokes shift ($\approx$10000 cm^{-1}). The species (I″) lacking intramolecular hydrogen bonding will exist only in solvents which are strong proton donor/acceptors, because of the competition with the intermolecular hydrogen bonding. ESIPT will not occur in species I″ due to the absence of direct path way for proton transfer between donor and acceptor groups. But non-observation of a large Stokes-shifted fluorescence band in o-APBO in cyclohexane, where the formation of species I′ will be more favourable than I or I″, could be due to a very low fluorescence quantum yield of species I′ and internal conversion

Table 2
Fluorescence band maxima (nm) and fluorescence quantum yields of 2-(aminophenyl) benzoxazoles in solvents of different polarity and at various acid concentrations

Solvent/species	o-APBO		m-APBO		p-APBO	
	λ_{max}	ϕ	λ_{max}	ϕ	λ_{max}	ϕ
cyclohexane	400 390(sh)	0.21	373	0.50	390 374 357 337	0.90
dioxane	410	0.80	395	0.40	390 375 360	1.05
acetonitrile	440sh 414	0.71	440(sh) 420	0.32	383	1.0
methanol	440(sh) 415	0.75	443	0.31	385	1.0
water (pH 6.9)	440(sh) 422	1.0	460	0.15	390	0.96
monocation	365	0.13	370	0.85	380	0.39
dication	440(sh) 400	0.63	393	0.73	440(sh) 395	0.72

Table 3
Stokes shift (cm^{-1}) observed in different solvents for o-APBO, m-APBO and p-APBO

Solvent	o-APBO	m-APBO	p-APBO
cyclohexane	3740	3960	2760
dioxane	4020	4990	3640
acetonitrile	4040	7640	4950
methanol	4150	8720	5280
water	5980	9910	5910

may be major path of deactivation as observed in other systems [1–3]. This is reflected by the low fluorescence quantum yield (0.21) of the normal Stokes-shifted band in cyclohexane compared to that (≈ 1.0) in water. Further basis for this assignment is as follows: (i) The full width at half maximum height of the fluorescence spectra is same in all the solvents, and (ii) the excitation spectra recorded by monitoring at 390 and 440 nm (assuming that the fluorescence bands originating from conformers I and I′ are mixed up with each other) in cyclohexane resemble the absorption spectrum.

The spectral changes observed in the different solvents are consistent with the nature of the basic substituents.

The larger blue shift in the absorption spectra of o-APBO compared to m-APBO and p-APBO is a consequence of the competition between the intra- and intermolecular HB in proton donor solvents. Since IHB is weak, as evidenced by IR data, it will be replaced by intermolecular hydrogen bonding in water. The increase of ϕ_f (table 2) with an increase in the solvent polarity also supports IHB in o-APBO. The intramolecular hydrogen bonding increases the rate of radiationless transitions, thus reducing ϕ_f. This explains the lower value of ϕ_f in cyclohexane and a higher one in water for o-APBO. Very large Stokes shift (table 3) observed in m-APBO with increase in the polarity of solvents indicates a large change in dipole moment and thus increase in the solvent interactions. The decrease in the fluorescence quantum yield of m-APBO in going from cyclohexane to water proves the effect of solvents on the spectral characteristics of m-APBO. Similar large Stokes shifts are also observed in m-HPBI in comparison with o-HPBI

Table 4
Electronic transitions (nm), polarisation of transition moment, charge densities at the various centres of hetero atoms in S_0 and S_1 states

Molecule	Transitions		Oscillator strength (calc.)	α [a] (deg)	Charge densities					
	obs.	calc.			S_0			S_1		
					O_1	N_3	N_{16}	O_1	N_3	N_{16}
p-APBO	325	324	1.261	352	1.816	1.307	1.934	1.857	1.319	1.915
	316			247						
	284	279		85						
	264	273								
m-APBO	325	319	1.076	352	1.815	1.302	1.937	1.857	1.320	1.936
	291	279	0.0568	296						
	248	273	0.104	257						
o-APBO (I″)	365	321	1.08	0	1.819	1.310	1.928	1.857	1.330	1.891
	348									
	297	274	0.1449	126						
	277	266	0.1294	255						
o-APBO (I)		324	1.05		1.815	1.405	1.925	1.852	1.445	1.891
		276	0.1293							
		271	0.1394							
o-APBO (I′)		439	0.584		1.853	1.688	1.406	1.852	1.647	1.230
		296	0.642							
		289	0.008							
		277	0.0272							

[a] α is the angle made by total transition moment vector with the positive direction of long axis (x axis).

[30] and *p*-HPBI [37] as well as in *m*-APBI [18] compared to *o*-APBI and *p*-APBI [18].

3.2. Effect of acid concentration

The absorption and fluorescence spectra of the molecules were studied in the H_0/pH/H_- range -10.4–16.0 and the spectral data are collected in tables 1 and 2. None of the molecules show any change of absorption characteristics in the region pH 14–5 indicating the presence of only neutral species. But the fluorescence intensity decreases at pH > 11 without the appearance of any new band. Since the monoanions, formed by deprotonation from $-NH_2$ group, with some exceptions [38], are in general, non-fluorescent [18,19] we attribute the decrease in fluorescence intensity to the formation of monoanion. A large blue shift in the absorption and fluorescence spectra at pH ≤ 4 indicates the formation of monocation (2). The monocation can be formed by protonation either at the ring nitrogen or at the $-NH_2$ group. Theoretical calculations (charge density data) as well as experimental results [16] ($pK_a(\geq N) \approx 5 \pm 0.5$, $pK_a(-NH_2) \approx 4 \pm 0.5$) have clearly established that the first protonation in case of amino-pyridines, quinoline [37] and benzimidazoles [18,30] takes place at the tertiary nitrogen atom. In our case, PPP calculations (table 4) have clearly indicated that the charge density at the tertiary nitrogen atom is much less than that at the amino-nitrogen. Consequently monocations will be formed by protonating the $-NH_2$ group. This is supported by the facts that (a) the pK_a value (0.0) of PBO [28] is much less than that of aniline (4.5) [39], and (b) the absorption and fluorescence band maxima of the monocations of *o*-APBO and *m*-APBO resemble that of PBO. A similar behaviour has also been observed in aminoindazoles [19].

In the absorption spectra of the monocation of *p*-APBO a weak band appears at 365 nm in addition to the main band at 295 nm. The presence of nice isosbestic points (297 nm, 368 nm) and the fact that

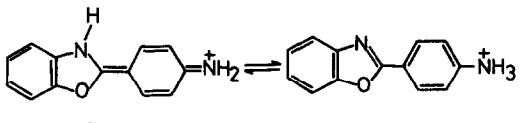

IV IV

Scheme 3.

the same pK_a values were obtained when the absorption intensity was monitored at 295 and 365 nm, ensures the existence of two species in the region pH 5.0–1.0. The longest wavelength band may arise from the contribution of the resonance form IV′ (scheme 3). A similar behaviour (i.e. red shift in absorption spectrum and blue shift in the fluorescence spectrum) has been observed during the first protonation of 2-aminobenzimidazole [18] and 2- and 4-aminoquinolines [40].

The red-shifted absorption (except for *p*-APBO monocation) and fluorescence spectra of the molecules at pH $\leqslant$ 0.5, which resemble the monocation spectrum of PBO (λ_a(mc) = 306 nm, λ_f(mc) = 385 nm), can be assigned to the dication (DCI), formed by protonation of the tertiary nitrogen. It is observed that the fluorescence intensity of the monocation (fig. 2) starts decreasing at pH 0.5 and a red-shifted fluorescence band starts appearing only at $H_0 - 1.0$. The decrease of fluorescence intensity of monocation without the appearance of any new band could be due to either proton induced fluorescence quenching or the formation of a new non-fluorescent species. We favour the latter and arguments in its support will be given later in proper place.

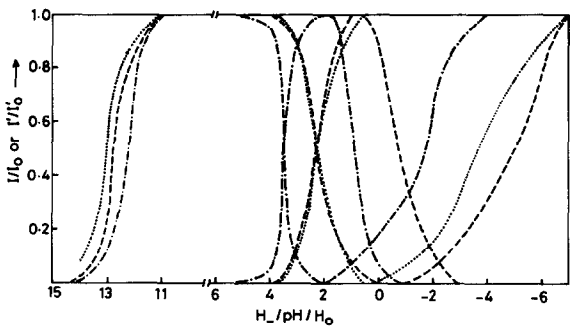

Fig. 2. Plot of the relative fluorescence intensity of the various prototropic species of *o*-APBO (---), *m*-APBO (–·–) and *p*-APBO (···) versus $H_-/pH/H_0$.

3.3. Acidity constants

The pK_a values for different prototropic reactions, determined using absorption data are listed in table 5. Since *p*-APBO is resonance stabilised, the electron density at the amino group will be decreased. Thus the pK_a value for the monocation–neutral equilibrium will be lower than that of *m*-APBO. The very low pK_a value for the dication–monocation equilibrium in *o*-APBO compared to other molecules is due to the presence of a nearby positive charge on the amino group which reduces the electron density at the pyridinic nitrogen atom.

The pK_a^* values for different prototropic equilibria have been determined by fluorimetric titrations (fig. 2) and Forster cycle method [38], wherever applicable. The pK_a^* values calculated by the Forster cycle method clearly indicate that the $-NH_2$ group becomes stronger acid upon excitation. Whereas the fluorimetric titrations have resulted in the ground state pK_a value for this equilibrium, indicating that the radiative decay rates for the conjugate acid–base pair are faster than the protonation/deprotonation rates. As a result the prototropic equilibrium is not established in the S_1 state. The large difference between the pK_a^* values for the moncation–neutral equilibrium in *m*-APBO calculated by using absorption and fluorescence data is, as mentioned earlier, due to difference in solvent relaxations for the conjugate acid–base pair in S_0 and S_1 states.

The Forster cycle method cannot be applied to calculate pK_a^* for dication–monocation equilibria of the molecules because of the formation of a species in the S_1 state which was not present in the S_0 state. The fluorimetric titration curves (fig. 2) do not show any correspondence between the decrease in the fluorescence intensity of monocation and increase in the fluorescence intensity of dication. Further, pK_a^* values determined from the formation curves of fluorimetric titrations for dication, have clearly indicated that the tertiary nitrogen atom becomes more acidic upon excitation which is opposite to that what is normally observed [39]. The foregoing facts and observations lead us to propose the formation of monocation (2′) formed as a result of biprotonic phototautomerism (scheme 4) in the S_1 state, i.e. a proton is dissociated from $-NH_3^+$ group and joins the tertiary nitrogen atom. Although as mentioned ear-

Table 5
Ground and excited state pK_a values for the various prototropic reactions of isomeric 2-(aminophenyl)benzoxazoles

Equilibrium	pK_a	pK_a^*		
		abs.	fluor.	F_1
o-APBO				
dication⇌monocation (2)	−2.0	–	–	–
dication⇌monocation (2′)	–	–	–	−5.0
monocation (2′)⇌monocation (2)	–	–	–	−0.7
monocation (2)⇌neutral	2.1	−5.8	−5.6	–
neutral⇌monoanion	>16	–	–	12.8
m-APBO				
dication⇌monocation (2)	−0.8	–	–	–
dication⇌monocation (2′)	–	–	–	−1.6
monocation (2′)⇌monocation (2)	–	–	–	0.9
monocation (2)⇌neutral	3.4	2.8	7.7	–
neutral⇌monoanion	>16	–	–	12.3
p-APBO				
dication⇌monocation (2)	−0.8	–	–	–
dication⇌monocation (2′)	–	–	–	−4.2
monocation (2′)⇌monocation (2)	–	–	–	–
monocation (2)⇌neutral	2.6	–	1.30	–
neutral⇌monoanion	>16	–	–	13.0

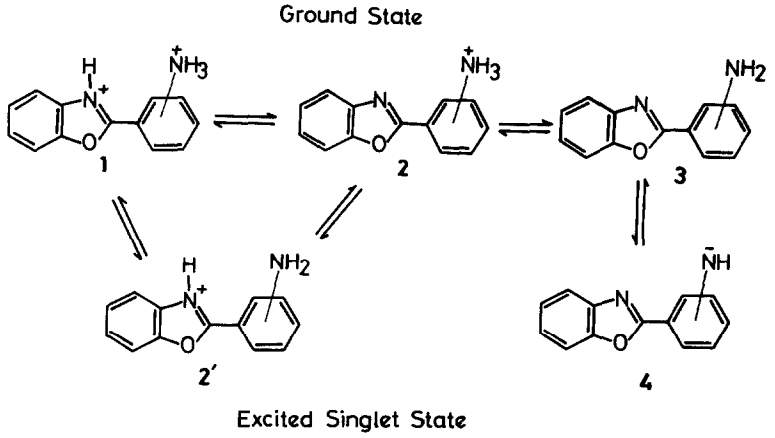

Scheme 4.

lier, the radiative decay rate in monocation (2) is faster than the rate of protonation/deprotonation at that pH, it may be possible that the rates are reversed when the acid concentration is increased. Further, it also appears that the fluorescence band maximum of species (2′) is not very different from that of either species (3) or (1) and the fluorescence quantum yield is very small. This is manifested by the large band width at half maximum in this acid range compared to other acid concentrations. Thus the decrease and increase in the fluorescence intensity of species (2) and dication (1) respectively represent the monocation (2′)–monocation (2) and dication (1)–monocation (2′) equilibria. Similar behaviour observed in

6-aminoindazole [19] indicates that the increase in the basicity of tertiary nitrogen atom and acidity of the $-NH_3^+$ group is such that the equilibrium is reversed in the S_1 state.

The fluorimetric titration curves at high basic strength are consistent with the literature results that the $-NH_2$ group becomes stronger acid in the S_1 state (table 5). Scheme 4 represents the various prototropic reactions occurring in S_0 and S_1 states.

3.4. Molecular orbital calculations

Molecular orbital calculations have been performed for all the molecules and different conformers of *o*-APBO, in the π-electron approximation introduced by Pariser, Parr and Pople [41–43] with a singly excited CI calculation. Parameters [44] used for the calculations are given in table 6. The molecules were assumed to be planar. All ring C–C, C–N and C–O bonds were taken to be 1.395 Å and standard values were used for other bonds. The ring systems were considered to be regular hexagon and pentagon. As suggested by Woolfe et al. [45], the IHB in *o*-APBO has been taken into account by lowering the value of core integral U_{kk} of the HB acceptor by 3 eV (in consistence with the known hydrogen bond strength). This places the U_{kk} of nitrogen atom approximately midway between those of pyrrolic and pyridinic nitrogen atoms.

The results of calculations are summarized in table 4. The calculated transition energies in all the cases are in good agreement with the observed values. Since we could not find the oscillator strengths (f) of different absorption bands, we are unable to compare the calculated f values. But qualitatively, the calculated f values are in consistence with the observed log ε values (table 1). The polarization of the transition moment corresponding to the long wavelength absorption band as mentioned earlier, is towards the phenyl ring. We have also calculated the π-electron density on the oxygen and nitrogen atom, sites involved in IHB in *o*-APBO. We have found that there is an increase of π-charge density on the tertiary nitrogen (N_3) on excitation. This makes the formation of the phototautomer I′ feasible in the S_1 state. It can also be found from table 4 that as expected, the π-charge density on amino nitrogen (N_{16}) is more than that on the pyridinic (N_3) nitrogen atom. Hence the monocation will be formed by protonation at the $-NH_2$ group. The calculated π-charge density on the $-NH_2$ group in the three molecules predicts that the pK_a values for the monocation–neutral equilibrium

Table 6
The parameters used in PPP calculations [a]

Atom, μ	I_μ (eV)	A_μ	Z_μ	ζ_μ	h_μ	$k_{\mu\nu}$
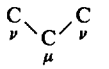	11.16	0.03	1	1.625	0.0	1.0
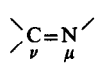	14.12	1.78	1	1.95	0.5	1.0
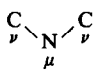	26.7	9.26	2	1.95	1.5	0.8
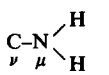	29.63	12.63	2	1.95	1.0	1.0
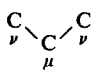	32.9	11.63	2	2.275	1.0	0.8

[a] I_μ and A_μ are valence state ionization potential and electron affinity of the atom μ respectively. Z_μ is the core charge at atom μ. ζ_μ is the orbital exponent. h_μ and $k_{\mu\nu}$ are defined by the relation $\alpha_\mu = \alpha_0 + h_\mu\beta_0$ and $\beta_{\mu\nu} = k_{\mu\nu}\beta_0$, where α_0 and β_0 are the Coulomb and resonance integrals respectively for carbon atom.

will be in order *o*-APBO, *p*-APBO, *m*-APBO. This is in good agreement with the results of table 5.

4. Conclusions

The following conclusions can be drawn from the above study: (i) Infrared, ultraviolet and fluorescence spectra, as well as the low pK_a value for the monocation–neutral equilibrium of *o*-APBO indicate the presence of intramolecular hydrogen bonding between the amino-proton and tertiary nitrogen atom. (ii) Only one normal Stokes-shifted fluorescence band, high fluorescence quantum yield, similar full width at half maximum height of the fluorescence band in all the solvents and similar fluorescence excitation spectra recorded at different fluorescence band maxima indicate that the rate of radiative decay of species I′ may be slower than that of internal conversion. (iii) The presence of vibrational structure in the spectral characteristics of *p*-APBO in moderately polar solvents could be due to the presence of dipolar structure III′. This is also manifested by the low pK_a value for the monocation–neutral equilibrium as well as by the absorption spectrum of the monocation of *p*-APBO. (iv) Increase in the basicity of the tertiary nitrogen atom and increase in the acidity of $-NH_3^+$ in the S_1 state lead to the formation of biprotonic phototautomer (2′).

Acknowledgement

We are thankful to the Department of Science and Technology, New Delhi, for the financial support to the project entitled "Proton transfer reactions in the excited states in the micellar media".

References

[1] J.R. Merrill and R. Bennett, J. Chem. Phys. 43 (1965) 1410.
[2] J.A. Otterstedt, J. Chem. Phys. 58 (1973) 5716.
[3] H. Shizuka, K. Matsui, T. Okamura and I. Tanaka, J. Phys. Chem. 79 (1975) 2731.
[4] W.F. Richy and R.S. Becker, J. Phys. Chem. 49 (1968) 2092.
[5] M.D. Cohen, G.M.J. Schmidt and S. Flavian, J. Chem. Soc. (1964) 2041;
M.D. Cohen, Y. Hirshberg and G.M.J. Schmidt, J. Chem. Soc. (1964) 2051, 2060;
M.D. Cohen and S. Flavian, J. Chem. Soc. B (1967) 317.
[6] R.S. Becker and W.F. Richy, J. Am. Chem. Soc. 89 (1967) 1298.
[7] A. Mordziński and A. Grabowska, Chem. Phys. Letters 90 (1982) 122.
[8] N.P. Ernsting, J. Phys. Chem. 89 (1985) 4932.
[9] A. Mordziński and W. Kuhnle, J. Phys. Chem. 90 (1986) 1445, 1455.
[10] K. Ding, S.J. Courtney, A. Strandjord, S. Flom, D. Friedrich and P.F. Barbara, J. Phys. Chem. 87 (1983) 1184.
[11] P.F. Barbara, P.M. Rentzepis and L.E. Brus, J. Am. Chem. Soc. 102 (1980) 2786.
[12] R.S. Becker, C. Lenoble and A. Zein, J. Phys. Chem. 91 (1987) 3509, 3517.
[13] K.P. Ghiggino, A.D. Scully and I.H. Lever, J. Phys. Chem. 90 (1986) 5089.
[14] G. Woessner, G. Goeller, J. Rieker, H. Hoier, J.J. Strezowski, E. Dattrozzo, M. Neureiter and H.E.A. Khamer, J. Phys. Chem. 89 (1985) 3629.
[15] T. Nishiya, S. Yamauchi, N. Hirota, M. Baba and I. Hamazaki, J. Phys. Chem. 90 (1986) 5730.
[16] A. Albert, R.J. Goldacre and J. Phillips, J. Chem. Soc. (1948) 2240;
A. Albert and R.J. Goldacre, J. Chem. Soc. (1943) 454; (1946) 706;
H.C. Longuet-Higgins, J. Chem. Phys. 18 (1951) 275.
[17] P.C. Tway and L.J. Clinelove, J. Phys. Chem. 86 (1982) 5223, 5227.
[18] A.K. Mishra and S.K. Dogra, Indian J. Chem. 24 A (1985) 815, 285; Indian J. Phys. 58 B (1984) 480; Bull. Chem. Soc. Japan 58 (1985) 3587.
[19] M. Swaminathan and S.K. Dogra, J. Am. Chem. Soc. 105 (1983) 6223;
A.K. Mishra and S.K. Dogra, Indian J. Chem. 24 A (1985) 364;
P. Phaniraj, A.K. Mishra and S.K. Dogra, Indian J. Chem. 24 A (1985) 913.
[20] D.W. Hein, R.J. Alheim and J.J. Leavitt, J. Am. Chem. Soc. 79 (1957) 427.
[21] J.A. Riddick and W.B. Bunger, Organic Solvents (Wiley–Interscience, New York, 1970) pp. 592–594, 798–805.
[22] R. Manoharan and S.K. Dogra, J. Phys. Chem. 92 (1988) 5282.
[23] R. Manoharan and S.K. Dogra, Can. J. Chem. 66 (1988) 2375.
[24] R. Manoharan and S.K. Dogra, J. Photochem. Photobiol. A 43 (1988) 81, 119.
[25] M. Krishnamurthy, H.K. Sinha and S.K. Dogra, Bull. Chem. Soc. Japan 60 (1987) 4401.
[26] R. Manoharan and S.K. Dogra, Bull. Chem. Soc. Japan 60 (1987) 4409.
[27] R. Passerini, J. Chem. Soc. (1954) 2256.
[28] J.K. Dey and S.K. Dogra, unpublished results.

[29] A.K. Mishra and S.K. Dogra, J. Photochem. 31 (1985) 333.
[30] H.K. Sinha and S.K. Dogra, Chem. Phys. 102 (1986) 337.
[31] M. Krishnamurthy and S.K. Dogra, J. Photochem. 32 (1986) 235, and references therein.
[32] M. Kamiya, Bull. Chem. Soc. Japan 43 (1970) 3344.
[33] A. Reisser, L.J. Leyshon, D. Saunders, M.V. Mijovic, A. Bright and J.J. Bogie, J. Am. Chem. Soc. 94 (1972) 2414.
[34] J. Roussille and N. Paillous, J. Chim. Phys. 80 (1983) 5957; S. Fery-Forques and N. Paillous, J. Org. Chem. 51 (1986) 672;
J. Roussille, F. Fargin, A. Lopez, B. Despax and N. Paillous, J. Org. Chem. 48 (1983) 3736.
[35] P. Brocklehurst, Tetrahedron 18 (1962) 299.
[36] R.N. Nurmukhamelov, G.V. Cobov and L.N. Phushkine, Russian J. Phys. Chem. 41 (1967) 831.
[37] H.K. Sinha and S.K. Dogra, J. Photochem. 36 (1987) 149.
[38] Th. Forster, Z. Elektrochem. 54 (1950) 42.
[39] J.F. Ireland and P.A.H. Wyatt, Advan. Phys. Org. Chem. 12 (1976) 132.
[40] P.J. Kovi, A.C. Capomacchia and S.G. Schulman, Anal. Chem. 44 (1972) 1611;
A.C. Capomacchia and S.G. Schulman, Anal. Chim. Acta 58 (1972) 91;
S.G. Schulman and L.P. Sanders, Anal. Chim. Acta 56 (1971) 83.
[41] R. Pariser and R.G. Parr, J. Chem. Phys. 21 (1953) 466, 767.
[42] J.A. Pople, Trans. Faraday Soc. 49 (1953) 1315.
[43] J. Delberne and H.H. Jaffe, J. Chem. Phys. 48 (1968) 1807, 4050.
[44] J. Hinze and H.H. Jaffe, J. Am. Chem. Soc. 84 (1962) 540.
[45] G.J. Woolfe, M. Melzig, S. Schneider and F. Dorr, Chem. Phys. 77 (1983) 213.